

A Fracture Mechanics approach to over-reinforced concrete beams

Alberto Carpinteri, Giuseppe Ferro & Giulio Ventura

Department of Structural and Geotechnical Engineering, Politecnico di Torino, Torino, Italy

ABSTRACT: Linear elastic fracture mechanics concepts are used to determine the equilibrium and compatibility equations of a beam segment subjected to bending in presence of a mode I edge crack. Recently, the model has been extended to include the presence of closing stresses as functions of the crack opening in addition to the steel reinforcement closing tractions. This aspect is particularly noteworthy and it has been proficiently used in the simulation and mechanical characterisation of high-performance and fibre-reinforced concrete members.

The problem of determining a limit to the compressive stresses in the concrete is introduced in this paper. In fact, when the beams are over-reinforced, collapse in compression occurs. This is formulated as an upper bound to the value of the brittleness number characterizing the bridged crack model. The upper bound to the reinforcement steel percentage inducing concrete crushing is consequently evaluated. When this bound is established by limit state analysis, it is restricted to absence of cohesive stresses. In the paper a general fracture mechanics model is presented for concrete crushing including the cohesive stresses contribution. The results are compared to the limit state analysis and to experimental results.

Keywords: Bridged Crack Model, Concrete crushing, Dimensionless parameters, LEFM, Size effects.

1 INTRODUCTION

There are several questions related to the use of the new-generation concretes. Among them, the high mechanical performances permit to consider larger and larger percentages of reinforcement. Fracture mechanics has been used for determining the minimum reinforcement for a concrete element in bending (Carpinteri 1981a; Carpinteri 1984), by considering the failure at the lower edge. The question arises whether it is possible to consider a Fracture Mechanics approach even for analyzing the collapse in compression. The complexity of the problem increases if the mechanical interaction of fibers added to the concrete matrix has to be accounted for. The bridged crack model has been originally proposed in (Carpinteri 1981a; Carpinteri 1984) and in (Bosco and Carpinteri 1995) for RC beams, reformulated in (Carpinteri and Massabó 1996; Carpinteri and Massabó 1997) for unreinforced concrete members with cohesive closing stresses and extended to the simultaneous presence of both steel and fibers reinforcements in (Carpinteri, Ferro, and Ventura 2003). The ability of dealing at the same time with steel reinforcements and closing stresses in the matrix results in a very flexible model, capable of modelling a wide range of quasi-brittle materials. Moreover, while limit state analysis yields only the ultimate load, the bridged crack model reveals also scale ef-

fects, instability phenomena and brittle-ductile transitions of the structural element.

In the paper the theoretical model is briefly recalled and the problem of introducing a limit to the compressive stresses in the concrete is addressed. This is accomplished by introducing the concept of nondimensional maximum compressive stress and determining influence functions based on LEFM. Consequently, an upper bound to the value of the brittleness number characterizing the bridged crack model is determined. The upper bound to the brittleness number can be immediately translated into a maximum percentage of reinforcement. Some experimental results are simulated and commented.

2 THE BRIDGED CRACK MODEL

The bridged crack model can be applied for evaluating the monotonic bending of a cracked reinforced concrete beam assuming as control parameter the crack depth at a given cross section. The model accounts for both the main reinforcement (steel bars) and a secondary reinforcement. The latter can be physically interpreted as the nonlinear tensile behavior of concrete due to the presence of reinforcement fibers.

Linear Elastic Fracture Mechanics is assumed for the matrix with a crack propagation condition ruled by the comparison of the stress-intensity fac-

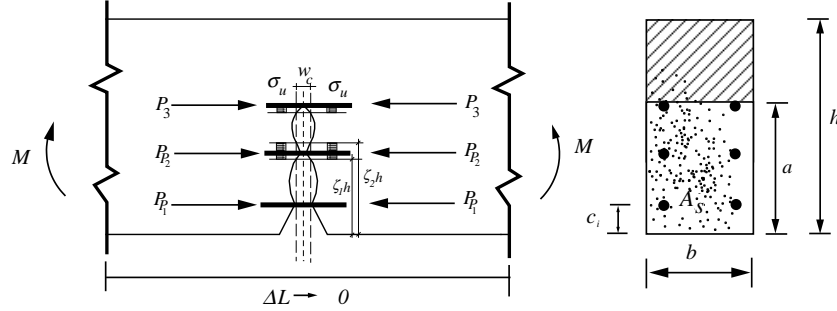


Figure 1: Model scheme of a cracked beam cross section.

tor K_I to the matrix fracture toughness K_{IC} . The stress-intensity factor is computed from the solutions reported in the stress-intensity factors handbooks (Okamura, Watanabe, and Takano 1975; Tada, Paris, and Irwin 1963).

The adopted model scheme is reported in Fig. 1 along with the used symbols: the section width b and height h , the crack depth a , the positions of the steel bars c and the relevant traction P_i . The geometric dimensions are converted into nondimensional quantities, after dividing by the height h . The nondimensional crack depth is denoted by $\xi = a/h$ and $\zeta = x/h$ represents the generic nondimensional abscissa from the bottom of the cross section.

The distributions of the discrete forces P_i and of the continuous ones σ applied to the crack surfaces represent the bridging mechanisms of the steel bars and of the cohesive stresses, respectively. The nondimensional position of the i -th steel reinforcement is denoted by $\zeta_i = c_i/h$, while $\sigma(w)$ represents the constitutive relation for the cohesive and/or fibers tractions, w being the crack opening at a generic position along the crack. Function $\sigma(w)$ is assumed to be zero for w greater than a critical value w_c . Its actual expression can be derived from experimental results or model codes. The constitutive relation for the reinforcement bars is assumed as rigid-plastic with no upper limit to deformation. The maxima of the bridging actions are defined by the ultimate traction $P_{P_i} = A_i \sigma_y$ in the bars and by the ultimate stress $\sigma_0 = \gamma \sigma_u$ for the fibers (or matrix), A_i being the i -th bar area, γ the volumetric percentage of fibers, σ_y and σ_u the minimum between yielding and sliding stress for the bars and fibers, respectively.

With reference to Fig. 1, let K_I be the stress-intensity factor at the crack tip. By the superposition principle, it is given by the sum of the stress-intensity factors K_{IM} due to the bending moment, K_{Ii} due to the m reinforcement bar tractions P_i and $K_{I\sigma}$ due to the distributed closing stresses $\sigma(w)$ along the crack

(Carpinteri, Ferro, and Ventura 2003; Ferro 2002):

$$K_I = K_{IM} - \sum_{i=1}^m K_{Ii} - K_{I\sigma}; \quad (1)$$

where the stress-intensity factors can be expressed in the form:

$$K_{IM} = \frac{M_F}{bh^{1.5}} Y_M(\xi); \quad (2)$$

$$K_{Ii} = \frac{P_i}{bh^{0.5}} Y_P(\xi, \zeta_i); \quad (3)$$

$$K_{I\sigma} = \sum_{i=1}^{n_c} h^{-0.5} \int_{\zeta_{1i}}^{\zeta_{2i}} \sigma_0(w(\zeta)) Y_P(\xi, \zeta) d\zeta; \quad (4)$$

and the functions Y_M and Y_P , are reported in (Okamura, Watanabe, and Takano 1975; Tada, Paris, and Irwin 1963; Carpinteri and Massabó 1996). In Eq. (4) n_c is the number of cohesive zones, where $\sigma_0(w) \neq 0$. These zones are defined over the intervals $[\zeta_{1i}, \zeta_{2i}]$, $i = 1 \dots n_c$.

Let ρ be the bar reinforcement percentage and define the brittleness numbers $N_P^{(1)}$, $N_P^{(2)}$ and the critical crack opening for the cohesive stresses \tilde{w}_c as:

$$N_P^{(1)} = \rho \frac{\sigma_y h^{0.5}}{K_{IC}} \quad ; \quad N_P^{(2)} = \gamma \frac{\sigma_u h^{0.5}}{K_{IC}}; \quad (5)$$

$$\tilde{w}_c = \frac{E w_c}{K_{IC} h^{0.5}}. \quad (6)$$

Substituting Eqs. (2,3,4) in (1), the following nondimensional equilibrium equation is obtained:

$$\tilde{M}_F = \frac{1}{Y_M(\xi)} \left(1 + N_P^{(1)} \sum_{i=1}^m \tilde{\rho}_i \tilde{P}_i Y_P(\xi, \zeta_i) + N_P^{(2)} \sum_{i=1}^{n_c} \int_{\zeta_{1i}}^{\zeta_{2i}} \tilde{\sigma}_0(\tilde{w}) Y_P(\xi, \zeta) d\zeta \right) \quad (7)$$

where:

$$\tilde{M}_F = \frac{M_F}{K_{IC}bh^{1.5}} \quad ; \quad \tilde{P}_i = \frac{P_i}{P_{P_i}} \quad (8)$$

$$\tilde{\rho}_i = \frac{\rho_i}{\rho} \quad ; \quad \tilde{\sigma}_0 = \frac{\sigma_0(w(\zeta))}{\gamma\sigma_u}. \quad (9)$$

The equilibrium equation (7) gives the propagation bending moment as a function of the bar traction and of the closing stresses. These quantities depend on the crack opening profile through the constitutive equations.

The crack opening at a general nondimensional abscissa ζ can be determined by summing the three contributions of the bending moment, bars traction and closing stresses. The nondimensional opening, evaluated at the crack propagation bending moment $M = M_F$, presents the following expression:

$$\begin{aligned} \tilde{w} &= \tilde{w}_M - \tilde{w}_P - \tilde{w}_\sigma = \\ & 2\tilde{M}_F \int_{\zeta}^{\xi} Y_M(x)Y_P(x, \zeta) dx + \\ & -2N_P^{(1)} \sum_{i=1}^m \tilde{\rho}_i \tilde{P}_i \int_{\max(\zeta, \zeta_i)}^{\xi} Y_P(x, z_i)Y_P(x, \zeta) dx + \\ & -2N_P^{(2)} \sum_{i=1}^{n_c} \int_{\zeta_{1_i}}^{\xi} \int_{h_1(\zeta)}^{h_2(x)} \tilde{\sigma}_0 Y_P(h_2(x), y) dy Y_P(x, \zeta) dx \quad (10) \end{aligned}$$

where:

$$h_1(\zeta) = \max(\zeta, \zeta_{1_i}); \quad h_2(x) = \min(x, \zeta_{2_i}). \quad (11)$$

By introducing the rigid-plastic constitutive equation for the bars, the displacement evaluated at $\zeta = \zeta_i$, $i = 1 \dots m$, equals zero if $P_{P_i} - P_i < 0$, i.e. if $1 - \tilde{P}_i < 0$. Let H be the Heaviside step-function. The diagonal matrix $[H_P] = \text{diag}(H(1 - \tilde{P}_i))$, $i = 1 \dots m$, allows for expressing the vector of the openings at the reinforcement bars as:

$$\{\tilde{w}\} = [H_P] \left(\{\tilde{\lambda}_M\} \tilde{M} - [\tilde{\lambda}] \{\tilde{P}\} - \{\tilde{w}_\sigma\} \right); \quad (12)$$

where the elements of the above vectors and matrices are $(i, j = 1 \dots m)$:

$$\{\tilde{\lambda}_M\}_i = 2 \int_{z_i}^{\xi} Y_M(x)Y_P(x, z_i) dx \quad (13)$$

$$[\tilde{\lambda}]_{ij} = 2N_P^{(1)} \tilde{\rho}_j \int_{\max(z_i, z_j)}^{\xi} Y_P(x, z_i)Y_P(x, z_j) dx \quad (14)$$

$$\{\tilde{w}_\sigma\}_i = \tilde{w}_\sigma(z_i). \quad (15)$$

Equation (12), with \tilde{M} given by (7), is a nonlinear integral equation in the unknowns \tilde{w} , n_c , $[\zeta_{1_i}, \zeta_{2_i}]$, $i = 1 \dots n_c$. Its solution for a given crack depth ξ allows for the determination of the opening function, the crack propagation bending moment \tilde{M}_F through (7) and the relative rotation of the cross section, given in nondimensional form by:

$$\begin{aligned} \tilde{\phi} &= \phi \frac{Eh^{0.5}}{K_{IC}} = \tilde{\phi}_M - \sum_{i=1}^m \tilde{\phi}_I - \tilde{\phi}_\sigma = \\ & = 2\tilde{M}_F \int_0^{\xi} Y_M^2(\zeta) d\zeta + \\ & -2N_P^{(1)} \sum_{i=1}^m \tilde{\rho}_i \tilde{P}_i \int_{z_i}^{\xi} Y_P(\zeta, z_i)Y_M(\zeta) d\zeta + \\ & -2N_P^{(2)} \sum_{i=1}^{n_c} \int_{\zeta_{1_i}}^{\xi} \int_{\zeta_{1_i}}^{h_2(x)} \tilde{\sigma}_0 Y_P(h_2(x), y) dy Y_M(x) dx \quad (16) \end{aligned}$$

with $h_2(x)$ given by Eq. (11).

3 CONCRETE CRUSHING AND MAXIMUM REINFORCEMENT

3.1 Problem statement by limit state analysis

In the limit state analysis, concrete crushing in bending is attained when the deformation reaches the critical value $\varepsilon_{cu} = 0.0035$. The nonlinear stress behavior in concrete is simplified assuming a rectangular stress block in compression, whose height is $0.8x$, x being the distance of the neutral axis from the upper edge of the rectangular section. The maximum compressive stress in concrete is given in this model by $0.85\sigma_{cu}$, where σ_{cu} is the compressive strength of concrete. This is illustrated in Figure 2, where all the quantities used in the present derivation are defined as well.

The following equations hold:

- linear deformation field

$$\varepsilon_s = \frac{d-x}{x} \varepsilon_{cu} \quad (17)$$

- equilibrium (rotation and translation)

$$\begin{aligned} M &= b 0.8x 0.85\sigma_{cu} (d - 0.4x) + \\ & - \sigma_s \eta A_s (d - z') \quad (18) \end{aligned}$$

$$\sigma_s A_s = b 0.85\sigma_{cu} 0.8x + \sigma_s \eta A_s \quad (19)$$

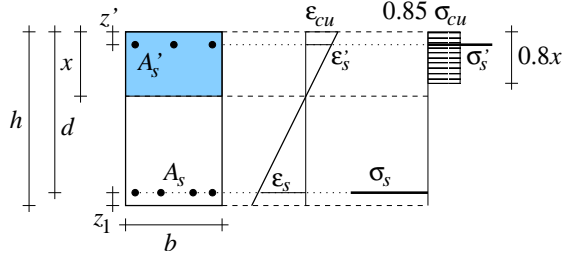


Figure 2: CEB-FIB model for a rectangular section in bending.

where $\eta = \frac{A'_s}{A_s}$. The steel bars are assumed to be linear elastic up to the yielding stress σ_y . Then, perfectly plastic behavior up to the rupture strain ε_{su} (usually $\varepsilon_{su} = 0.01$) is assumed.

The problem (17,18,19) has a solution only for a tension reinforcement area greater than a minimum value A_{sc} to be determined. Moreover, for any $A_s > A_{sc}$, a different value of the bending moment M at crushing is obtained, M being a monotonically increasing function of the neutral axis coordinate x .

As a consequence, because of the equilibrium, the bending moment at concrete crushing is a monotonically increasing function of the tension reinforcement area A_s . The minimum bending moment producing the crushing collapse of concrete is therefore obtained when the maximum allowable strain ε_{su} in the tension reinforcement is present. This condition is assumed here, being both a safe and optimal design condition at the same time.

It will be therefore assumed $A_s = A_{sc}$. The value of A_{sc} can be computed by the condition that the deformation and stress in the tension steel are the rupture ones, i.e. $\varepsilon_s = \varepsilon_{su}$, $\sigma_s = \sigma_y$. From Eq. (17), the neutral axis coordinate is determined as:

$$x = \frac{\varepsilon_{cu}}{\varepsilon_{su} - \varepsilon_{cu}} h, \quad (20)$$

and, upon substitution of the usual values for the maximum deformations,

$$x = 0.259 h \quad (21)$$

A final consideration holds for the stresses in the compression reinforcement steel. It is observed that for usual beam geometries ($z' \ll h$) and steel type, the compression reinforcement yields significantly before concrete crushing, so that $\sigma'_s = \sigma_y$ can be assumed.

The minimum reinforcement area inducing concrete crushing failure is obtained after substitution of Eq. (21) into Eq. (19)

$$A_{sc} = \frac{0.176}{1 - \eta} b d \frac{\sigma_{cu}}{\sigma_y} ; \quad \eta < 1. \quad (22)$$

From this equation, observing that $h = d + z_1$ and dividing by bh both terms, the critical reinforcement

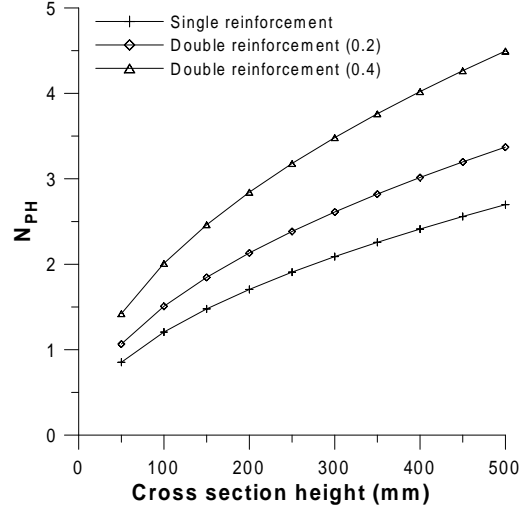


Figure 3: Maximum brittleness number for single and double reinforced beams. The reinforcement ratio η is reported within parentheses.

ratio ρ_{sc} is obtained and, upon substitution into the brittleness number definition, it follows:

$$N_{PH}^{(1)} = 0.176 \frac{1 - \zeta_1}{1 - \eta} \frac{\sigma_{cu} h^{0.5}}{K_{IC}} ; \quad \eta < 1. \quad (23)$$

In Figure 3 a plot of $N_{PH}^{(1)}$ is reported, assuming the data $\sigma_{cu} = 48.2 \text{ Nmm}^{-2}$, $K_{IC} = 63.4 \text{ Nmm}^{-3/2}$, $\zeta_1 = 0.1$, $\eta = 0, 0.2, 0.4$, by varying the cross section height between 50 and 500 mm.

3.2 Problem statement by fracture mechanics

By the superposition principle, the stress state at the upper edge of the cracked section can be written as the sum of the contribution due to the bending moment and the one of the forces acting on the crack edges

$$\sigma_c = \sigma_c^M + \sum_{i=1}^m \sigma_c^{P_i} + \sigma_c^\sigma. \quad (24)$$

By introducing two new nondimensional functions Y_σ^M and Y_σ^P , the contributions can be written as:

$$\sigma_c^M = \frac{M}{bh^2} Y_\sigma^M(\xi) \quad (25)$$

$$\sigma_c^{P_i} = \frac{P_i}{bh} Y_\sigma^P(\xi, \zeta_i) \quad (26)$$

$$\sigma_c^\sigma = \frac{1}{bh} \sum_{i=1}^{n_c} \int_{\zeta_{1_i}}^{\zeta_{2_i}} \sigma_0(w(y)) Y_\sigma^P(\xi, y) dy. \quad (27)$$

To rewrite Eqs. (25, 26, 27) in nondimensional form, the definition of brittleness numbers and of nondimensional bending moment $M = \tilde{M} K_{IC} b h^{1.5}$ and traction $P_i = \tilde{P}_i b h \sigma_y \rho_i$ are introduced:

$$\sigma_c^M = \frac{K_{IC}}{h^{0.5}} Y_\sigma^M(\xi) \tilde{M} \quad (28)$$

$$\sigma_c^{P_i} = \frac{K_{IC}}{h^{0.5}} N_P^{(1)} \frac{\rho_i}{\rho} Y_\sigma^P(\xi, \zeta_i) \tilde{P}_i \quad (29)$$

$$\sigma_c^\sigma = N_P^{(2)} \frac{K_{IC}}{b h^{1.5}} \sum_{i=1}^{n_c} \int_{\zeta_{1i}}^{\zeta_{2i}} \tilde{\sigma}_0(w(y)) Y_\sigma^P(\xi, y) dy. \quad (30)$$

Consequently, the following nondimensional stresses $\tilde{\sigma}_c$ are defined:

$$\tilde{\sigma}_c^M = \sigma_c^M \frac{h^{0.5}}{K_{IC}} = Y_\sigma^M(\xi) \tilde{M} \quad (31)$$

$$\tilde{\sigma}_c^{P_i} = \sigma_c^{P_i} \frac{h^{0.5}}{K_{IC}} = N_P^{(1)} Y_\sigma^P(\xi, \zeta_i) \tilde{\rho}_i \tilde{P}_i \quad (32)$$

$$\begin{aligned} \tilde{\sigma}_c^\sigma &= \sigma_c^\sigma \frac{b h^{1.5}}{K_{IC}} = \\ &= N_P^{(2)} \sum_{i=1}^{n_c} \int_{\zeta_{1i}}^{\zeta_{2i}} \tilde{\sigma}_0(w(y)) Y_\sigma^P(\xi, y) dy, \end{aligned} \quad (33)$$

and Eq. (24) can be expressed in nondimensional form:

$$\tilde{\sigma}_c = \tilde{\sigma}_c^M + \sum_{i=1}^m \tilde{\sigma}_c^{P_i} + \tilde{\sigma}_c^\sigma. \quad (34)$$

The determination of the functions Y_σ^M and Y_σ^P is carried out by finite elements analysis and applying a nonlinear regression to the numerical data. A cracked beam segment is considered, subjected to a bending moment at the ends or to two opposite forces along the crack edges. In these two configurations, the stress σ_c is evaluated discretizing half of the beam and using adaptive meshing.

The two evaluated functions are:

$$\begin{aligned} Y_\sigma^M(\xi) &= -5.997 + 3.269\xi - \frac{5.400\xi}{(1-\xi)^2} + \\ &- 16.311\xi^2 - 3.721\xi^3 \end{aligned} \quad (35)$$

$$\begin{aligned} Y_\sigma^P(\xi, z) &= \frac{\xi - z}{(1-\xi)^2} (-10.286 + 10.959\xi + \\ &- 6.112\xi^2 - 9.574z + 13.509\xi z - 3.835z^2) \end{aligned} \quad (36)$$

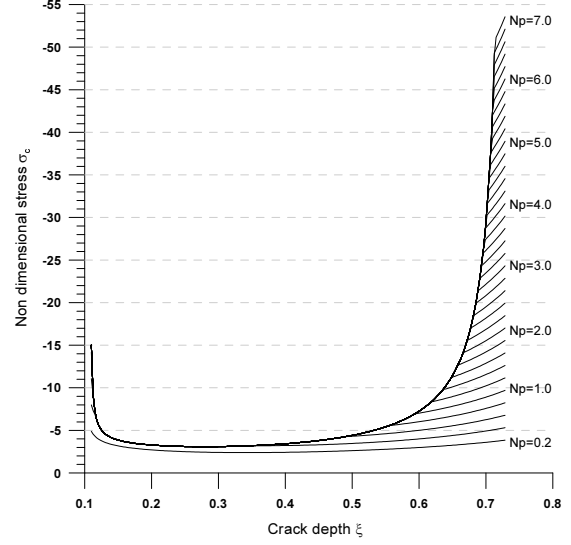


Figure 4: nondimensional maximum compressive stress in the upper part of the cross section as a function of the crack depth ξ .

The above development allows for evaluating the maximum compressive stress in concrete, considering the effect of closing stresses distributed on the crack faces. In the following, it will be shown how this allows to define an upper bound to the brittleness numbers.

On the other hand, the model allows also the determination of the minimum reinforcement so that the rupture is ductile. This has been determined under the hypothesis of absence of cohesive stresses ($N_P^{(2)} = 0$) in (Bosco and Carpinteri 1992), where the Authors obtained the following relation between the minimum brittleness number $N_{PC}^{(1)}$ and the compressive strength of concrete:

$$N_{PC}^{(1)} = 0.1 + 0.0023\sigma_{cu} \quad (37)$$

σ_{cu} being expressed in N/mm^2 . A beam having a brittleness number lower than the limit expressed by Eq. (37) exhibits a brittle failure because of insufficient reinforcement. In this case, when the crack develops at the lower edge and crosses the reinforcement, the latter is immediately yielded and strained to rupture, so that the peak load is higher than the yielding branch.

Consequently, a region of brittleness number values where a beam presents ductile behavior is easily defined:

$$N_{PC}^{(1)} < N_P^{(1)} < N_{PH}^{(1)} \quad (38)$$

A plot of the nondimensional stresses, Eq. (34), versus the crack depth ξ is shown in Fig. 4. For the sake of comparison to experimental results presented in

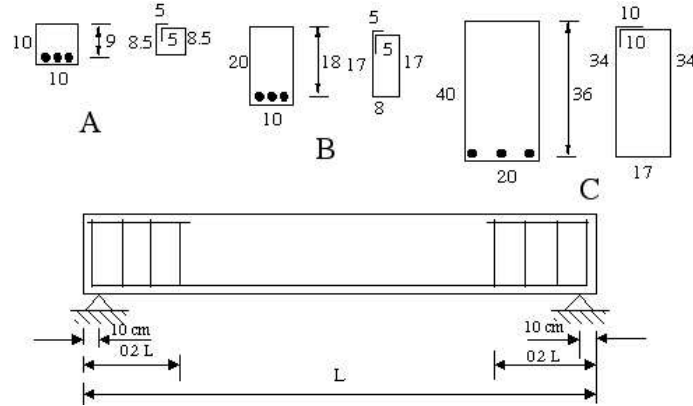


Figure 5: Geometry of the beams tested by Carpinteri et al. (1999).

the next section, the figure refers to the case where no distributed closing stresses are present, i.e. $N_P^{(2)} = 0$, $N_P = N_P^{(1)} \neq 0$. The curves present a slope discontinuity when yielding of the reinforcing bars occurs. In the following section it will be shown how the upper limit N_{PH} , Eq. (38), can be derived from Fig. 4 with reference to experimental results. The value N_{PH} represents the upper bound of applicability for the bridged crack model for beams with single or double reinforcement. Beams having $N_P^{(1)} > N_{PH}$ will exhibit crushing failure.

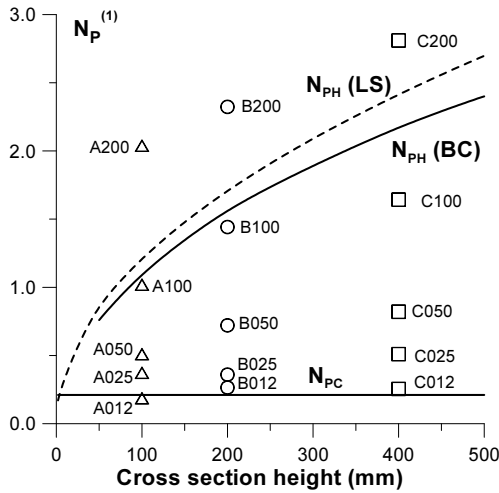


Figure 6: Brittleness numbers for the tested beams and limit curve of concrete crushing N_{PH} .

4 EXPERIMENTAL RESULTS

The behavior predicted by inequality (38) has been confirmed by the experimental results provided by Bosco and Carpinteri (Carpinteri, Ferro, Bosco, and Elkatieb 1999). The Authors examine three series of

reinforced beams by varying the cross section and the reinforcement area. The tests were performed on 35 beams of classes A, B and C, with cross-sectional area equal to 100×100 , 100×200 and 200×400 mm, respectively (Fig. 5), and concrete properties $\sigma_{cu} = 48.2 \text{ Nmm}^{-2}$, $K_{IC} = 63.4 \text{ Nmm}^{-3/2}$. The examined reinforcement percentages are 0.12%, 0.25%, 0.50%, 1.00%, 2.00%. The beams are labelled with the letter of the series, the reinforcement percentage and, occasionally, with the slenderness ratio L/h , e.g. A025-6 means a series A beam with 0.25% reinforcement and $L/h = 6$. In Fig. 6 the brittleness numbers computed for the experimental tests are plotted together with the value of N_{PC} , Eq. (37), and the curves of N_{PH} computed by a limit state analysis, $N_{PH}(LS)$, and by the bridged crack model, $N_{PH}(BC)$. The latter curve, $N_{PH}(BC)$, has been derived from Figure 4. In fact, in the present case, the maximum nondimensional stress in concrete as a function of the cross section height is given by:

$$\tilde{\sigma}_c = \frac{\sqrt{h}}{K_{IC}} \sigma_c \quad (39)$$

In Fig. 7 the nondimensional maximum stress value, computed with the above material data and cross section heights $h = 50, 100, 200, 300, 400, 500$ mm, intersects the ξ vs. $\tilde{\sigma}_c$ curves. The $\tilde{\sigma}_c$ curves are drawn for several values of $N_P^{(1)}$, and each one presents a slope discontinuity when the steel reinforcement yields. Then, for a given height, the limit condition occurs when at the same time the maximum value of $\tilde{\sigma}_c$ is attained and the reinforcement yields. The brittleness number in this situation is N_{PH} and has been determined graphically from the family of curves obtained varying $N_P^{(1)}$ (Fig. 7). These values are plotted in Fig. 6 as the solid curve $N_{PH}(BC)$. The comparison to the limit analysis approach (dashed line) evidences a similar trend, but the Bridged Crack model

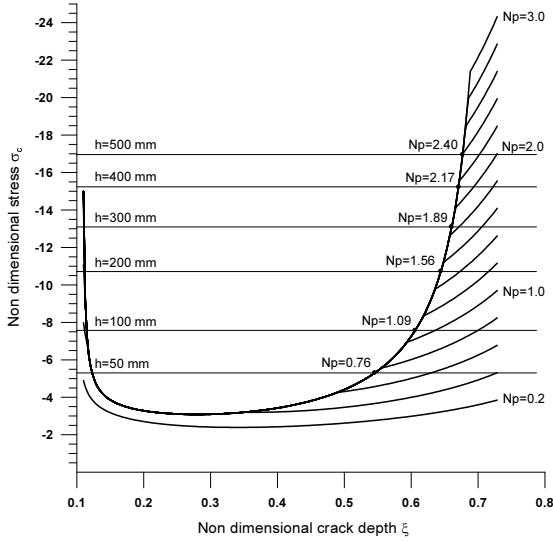


Figure 7: Determination of the brittleness number N_{PH} .

is able to account for the presence of fibers or cohesion of the matrix and its different dimensional effect, Eqs. (33). This topic is currently under development.

The experimental results confirm that all the beams above the N_{PH} curve failed because of concrete crushing, while the beams with $N_P < N_{PC}$ failed for insufficient reinforcement. All the above concepts about minimum and maximum brittleness number $N_P^{(1)}$ can be immediately translated into minimum and maximum reinforcement area. Considering the data from Fig. 7 and Eq. (37), two curves are determined enclosing the reinforcement percentages for a given section height so that the mechanical behavior is ductile. This is shown in Fig. 8 for both the limit state analysis (LS, dashed curve) and bridged crack (BC, solid curve) approaches. The small oscillations observed in the figure are due to the graphical procedure used to extract the N_{PH} values from the parametric curves in Fig. 7.

Finally, for some beams of the series B and C the load–displacement curves have been simulated by the bridged crack model. The model provides the values of the nondimensional bending moment and rotation as functions of the crack depth. For comparison with the experimental results, these values have been converted into displacement versus load diagrams. The displacement at midspan of the beam is supposed given by the elastic part plus a rigid part due to the localised rotation of the cracked section. From the definition of nondimensional bending moment and rotation, we can write:

$$M_F = \tilde{M} K_{IC} b h^{1.5}, \quad \phi = \frac{\tilde{\phi} K_{IC}}{E^* h^{0.5}}. \quad (40)$$

Consequently, the vertical load and displacement at

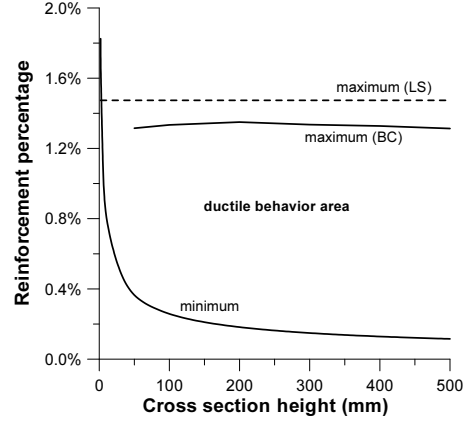


Figure 8: Reinforcement percentages for ductile cross sections according to limit state (LS) and bridged crack (BC) approaches.

midspan are given by:

$$P = \frac{4M_F}{L}, \quad (41)$$

$$\delta = \delta_{el} + \delta_{\phi} = M_F \frac{L^2}{48E^*I} + \frac{\phi L}{4}, \quad (42)$$

where the inertia is related to the total cross section, L is the span length, and $E^* = E/2.2$, E being the conventional 28 days static modulus. This assumption is already present in the literature (Carpinteri 1981b; Jenq and Shah 1986) and takes into account the nonlinear material behavior in the zone ahead of the crack tip. The experimental and computational load vs. deflection diagrams are reported in Figs. 9 and 10. The numerical simulation was carried out assuming the data reported in (Carpinteri, Ferro, Bosco, and Elkatieb 1999). The model is of course not able to reproduce the progressive decrease in the tangent modulus due to concrete damage and to the formation of further additional cracks along the span. This effect is particularly marked in these experimental tests, while much closer results for the load–displacement curves were obtained in the simulation of other results, e.g. (Swamy and Al-Ta’an 1981) as reported in (Carpinteri, Ferro, and Ventura 2003). Although the deflection is not closely reproduced due to diffuse cracking, the model is able to simulate the mechanical behavior of the beams, and noticeably the initially unstable behavior of the ones with the lowest reinforcement percentage (B025, C025), the steel yielding collapse of the beams B100 and C100, and the concrete crushing collapse of the beams B200 and C200.

5 CONCLUSIONS

The bridged crack model has been recently extended to the simultaneous presence of embedded conven-

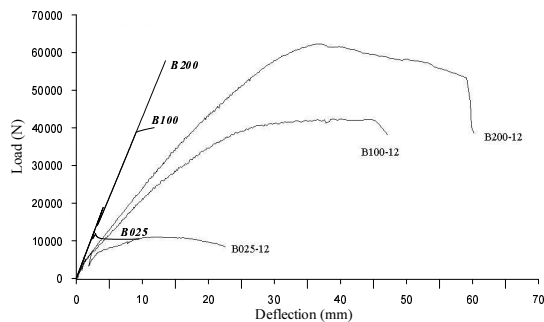


Figure 9: Experimental and computational load vs. deflection diagrams for the series B12 beams.

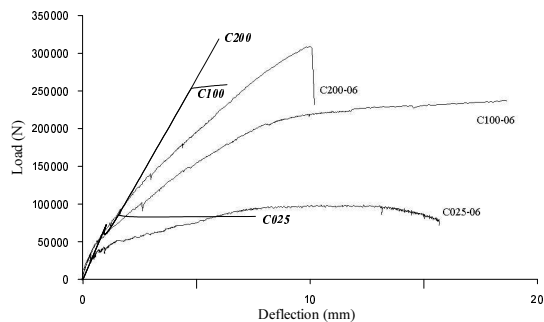


Figure 10: Experimental and computational load vs. deflection diagrams for the series C6 beams.

tional steel bar reinforcements and fibers mixed into the cementitious matrix. The two reinforcements act at different scales and influence each other in the global structural response. Compared to classical limit state analysis, the introduction of Fracture Mechanics concepts into the modelling of reinforced concrete members allows for determining ductile-brittle transitions, scale effects and the contribution of fibers and, in general, nonlinear matrix tensile behavior. Crushing of concrete is introduced in the model by determining an upper bound to the brittleness number. When coupled to the results presented for the minimum reinforcement (Carpinteri, Ferro, Bosco, and Elkatieb 1999), this defines a ductility domain. The ductility domain allows for designing the collapse mechanism for a beam in bending by simply evaluating its brittleness number. This extension of the model is here presented in the general case of simultaneous presence of fibers and steel reinforcement bars. It is however tested in the case of conventional steel bar reinforcement due to limitations in the availability of experimental data.

ACKNOWLEDGEMENTS:

The present research was carried out with the fi-

ancial support of the Ministry of University and Scientific Research (MIUR) and the National Research Council of Italy (CNR). Financial support from the European Union, TMR Contract ERBFMRXCT960062, is also gratefully acknowledged.

REFERENCES

- Bosco, C. and A. Carpinteri 1992. Softening and snap-through behavior of reinforced elements. *J. Eng. Mechanics (ASCE)* 118, 1564–1577.
- Bosco, C. and A. Carpinteri 1995. Discontinuous constitutive response of brittle matrix fibrous composites. *Journal of the Mechanics and Physics of Solids* 43, 261–274.
- Carpinteri, A. 1981a. A fracture mechanics model for reinforced concrete collapse. In *Proceedings of the I.A.B.S.E. Colloquium on Advanced Mechanics of Reinforced Concrete*, Delft, pp. 17–30.
- Carpinteri, A. 1981b. Static and energetic fracture parameters for rocks and concrete. *Materials and Structures* 14, 151–162.
- Carpinteri, A. 1984. Stability of fracturing process in rc beams. *Journal of Structural Engineering (ASCE)* 110, 544–558.
- Carpinteri, A., G. Ferro, C. Bosco, and M. Elkatieb 1999. Scale effects and transitional failure phenomena of reinforced concrete beams in flexure. In A. Carpinteri (Ed.), *Minimum Reinforcement in Concrete Members*, Volume 24 of *ESIS Publications*, pp. 1–30. Elsevier Science Ltd.
- Carpinteri, A., G. Ferro, and G. Ventura 2003. Size effects on flexural response of reinforced concrete elements with a nonlinear matrix. *Engineering Fracture Mechanics* 70, 995–1013.
- Carpinteri, A. and R. Massabó 1996. Bridged versus cohesive crack in the flexural behavior of brittle-matrix composites. *International Journal of Fracture* 81, 125–145.
- Carpinteri, A. and R. Massabó 1997. Continuous vs discontinuous bridged-crack model for fiber-reinforced materials in flexure. *International Journal of Solids and Structures* 34, 2321–2338.
- Ferro, G. 2002. Multilevel bridged crack model for high-performance concretes. *Theoretical and Applied Fracture Mechanics* 38, 177–190.
- Jenq, Y. and S. Shah 1986. Crack propagation in fiber-reinforced concrete. *Journal of Engineering Mechanics (ASCE)* 112, 19–34.
- Okamura, H., K. Watanabe, and T. Takano 1975. Deformation and strength of cracked member under bending moment and axial force. *Engineering Fracture Mechanics* 7, 531–539.
- Swamy, R. and S. Al-Ta'an 1981. Deformation and ultimate strength in flexure of reinforced beams made with steel fiber concrete. *ACI Journal* 5, 395–405.
- Tada, H., P. Paris, and G. Irwin 1963. *The Stress Analysis of Cracks Handbook*. St. Louis, Missouri: Paris Productions Incorporated (and Del Research Corporation).